ABSTRACT

LEVEDAHL, BLAINE ALEXANDER. Decentralized Autonomous Control of Aerospace Vehicle Formations. (Under the direction of Dr. Larry Silverberg).

Two approaches for the autonomous control of aerospace vehicle formations are developed. The development of the approaches relies on fundamental work in the areas of distributed control; specifically modal, robust, optimal, and decentralized control. The algorithms are shown to satisfy five separation principles that simplify design and enable the algorithms to be implemented reliably. The autonomous controllers uniformly dampen the modes of the formation (global control) using a decentralized approach and a nearest-neighbor approach. A numerical example illustrates robust formation changes from 9-vehicle (3 x 3) grids to V-type formations.

DECENTRALIZED AUTONOMOUS CONTROL OF AEROSPACE VEHICLE FORMATIONS

by

Blaine Alexander Levedahl

A thesis submitted to the Graduate Faculty of
North Carolina State University in partial
fulfillment of the requirements for the Degree of
Master of Science

Aerospace Engineering

Raleigh, North Carolina

2003

Approved by:

Dr. Ashok Gopalarathnam	Dr. Edward Grant

Dr. Larry Silverberg, Chair of Advisory Committee

BIOGRAPHY

The author, Blaine Alexander Levedahl, was born in Manchester, Connecticut on July 2, 1976 to Joseph William and Alexandria Mentschikoff Levedahl. At an early age, Blaine became interest in architecture after being influenced by Frank Lloyd Wright. In high school, he pursued this desire by taking numerous mechanical and architectural drafting classes. By graduation, Blaine had developed a desire to study the most sophisticated of machines, the aircraft. During his pursuit to obtain his undergraduate degree in aerospace engineering from North Carolina State University he developed a love for the Japanese language and culture. In the summer of 1998 he had the opportunity to study at Waseda University in Tokyo which solidified his desire to minor in Japanese. During Blaine's senior year, he met Akiko Takamatsu who has since become his loving and supportive wife. Upon graduation, Blaine received admission to North Carolina State University's Master's in Aerospace Engineering Program and a NASA Fellowship for full funding of his research and graduate study. Under the direction of Dr. Larry Silverberg, at NCSU, and David Cox, at NASA Langley Research Center, Blaine has conducted the research here in.

ACKNOWLEDGEMENTS

The author wishes to express his sincere appreciation to Dr. Larry Silverberg who not only imparted his expertise, but also offered fatherly advice on many life issues the author experienced. The lessons learned and conversations had will be something the author will prize for his days to come. The author would also like to thank the graduate committee, Dr. Ashok Gopalarathnam who introduced the author to the field of aircraft controls and Dr. Edward Grant of the Electrical and Computer Engineering Department, for their insightful questions and assistance.

The author would also like to express appreciation to David Cox at NASA Langley Research Center for the opportunities, experiences, and support that he has extended. It has been an honor and an unparalleled learning experience to work with David.

The author would also like to thank his family. His grandmother, Soia Mentschikoff, even after her passing, has continued her teachings and support. His mother, father, and stepmother, Alexandria Mentschikoff Levedahl, Dr. Joseph William Levedahl, and Jae-Shin Yang have always supported his interests and goals no matter how eccentric. His siblings, Katie and Peter, have always given rapid feedback even on the most mundane of issues. His wife, Akiko Takamatsu, has shown infinite patience and support in all his endeavors and continues to be his stimulus to persevere through difficult times.

菅原道真先生は私に研究において進むべき道を示してくださいました。感謝しています。どうもありがとうございました。

Thank you all very much.

TABLE OF CONTENTS

LIST OF TABLES

LIST OF FIGURES

GLOSSARY

Decentralized. Using inertial sensing measurements, such as GPS, to give global position measurements for each vehicle in the formation. Gives information for both tracking and regulation control.

Elementary Formation. A set of formations, for classification purposes, involving a few vehicles that can be used to build more complex formations. Useful in reducing the transmission information required for a specific formation change.

Nearest Neighbor. Using relative sensing measurements, such as sensing truss, to give relative position measurements between 2 vehicles in the formation. Gives information for regulation control only.

Parabolic Eccentricity. Ratio of the length to the height of a vehicles parabolic trajectory in a 2-dimension formation change. Similar parameters can be set up for more complex paths and for 3-dimensions.

Regulation Control. Type of control associated with maintaining a vehicle in the neighborhood of an equilibrium. Regulation control includes suppressing vibration, damping, stiffening, isolating, and complying.

Sensing Truss. A sensing method using an arrangement of transmitters and receivers for the relative measurement between 2 vehicles. The sensing truss possesses stability characteristics analogous to the stability characteristics of the corresponding structural truss.

Separation Principles. Principles that allow certain design steps to be performed independent of one another. For example, tracking and regulation control, transmitting and receiving signals, and spatial and temporal tracking.

Tracking Control. Type of control associated with moving a vehicles form one equilibrium to another. Tracking control includes repositioning, placing, turning, switching, and changing formation.

Chapter 1

INTRODUCTION

The autonomous control of aerospace vehicle formations is a new and important upcoming vehicle control problem in the aerospace industry. The problem is motivated by the recent successes of Unmanned Aerial Vehicle (UAV) technology and represents a relatively new application to fundamental issues in distributed control, sensing, and electronics. The strategy employed to solve this control problem builds on the already strong foundation that exists in several primary areas of distributed control, namely, modal control, robust control, decentralized control, and optimal control. Pioneering work in Modal Control had appeared by Balas[1] in 1978, and by Meirovitch and Baruh[2] in 1982. A strong framework for robust control of self-adjoint, distributed-parameter systems was developed by Arbel and Gupta[3] in 1981, by Hale and Rahn[4] in 1984, and the robust control problem was applied to Modal Control by Baruh and Silverberg[5] in 1985. Calico and Miller[6] in 1983 were among the first to formulate the decentralized control problem for self-adjoint distributed systems.

An important outcome of the research in distributed control during the 1970s and 1980s was the recognition that modal control, optimal control, decentralized control, and robust control were not necessarily conflicting objectives. Modal Control was formulated as a globally optimal control problem by Meirovitch and Silverberg[7] in 1986, and the first-order approximation to this globally optimal control problem was shown to be decentralized by Silverberg[8] in 1985. This mutually optimal, modal, decentralized, and robust control was examined in more detail by Silverberg and Morton[9] in 1989, by Silverberg[10] in 1990, and by Silverberg, Redmond and Weaver[11] in 1992. The application of these results to maneuvering spacecraft was developed by Baruh and Silverberg[12]

in 1988 and by Silverberg and Foster[13] in 1990. It was shown that the mutually optimal, modal, decentralized, robust control indicated above could uniformly dampen and uniformly stiffen the modes of vibration of the distributed system by Silverberg and Washington[14,15] in 1997 and 1999.

The application of decentralized control to autonomous formations has also received some attention. Wolfe, Chichka, and Speyer used a vortex lattice method and decentralized regulation of a 3 plane V formation[16]. The re-calculation of the stability derivatives in tight formations was considered by Pachter, D'Azzo, and Proud[17]. This thesis presents one of many strategies that can be employed to autonomous control (tracking and regulation) of vehicle formations. The strategy developed in this thesis places an emphasis on good design practices, specifically on the goal of separating the problem into independent effects at the controls, sensors, and electronics levels.

Chapter 2 formulates the problem and Chapter 3 discusses the communication and measurement requirements. Chapter 4 formulates the problem of changing the formation and Chapter 5 formulates the problem of maintaining the formation, in which a decentralized control strategy and a nearest-neighbor control strategy are used. Chapter 6 provides a numerical example that brings out basic features of the autonomous controls and Chapter 7 concludes.

Chapter 2

PROBLEM FORMULATION

Consider a formation of n rigid vehicles. The i^{th} vehicle is governed by the six equations

$$\begin{aligned} m^{(i)}\ddot{\mathbf{r}}^{(i)} &= \mathbf{F}_C^{(i)} + \mathbf{F}_D^{(i)}, \\ I^{(i)}\dot{\boldsymbol{\omega}}^{(i)} + \boldsymbol{\omega}^{(i)} \times I\boldsymbol{\omega}^{(i)} &= \mathbf{M}_C^{(i)} + \mathbf{M}_D^{(i)}, \\ \text{where, } (i &= 1, 2, \ldots, n) \end{aligned} \tag{1}$$

in which m is mass, $\mathbf{r}$ is the position vector of the mass center, $\mathbf{F}_C$ is the control force vector, $\mathbf{F}_D$ is the disturbance force vector, I is the inertia matrix about the mass center, $\boldsymbol{\omega}$ is the angular velocity vector, $\mathbf{M}_C$ is the control moment about the mass center, $\mathbf{M}_D$ is the disturbance moment about the mass center, and where over-dots indicate time differentiation. The following developments apply to a wide range of vehicle types, e.g. balloons, aircraft, spacecraft, submersibles, and automobiles. Regardless of the vehicle type, vehicle control and formation control can be partitioned into separate problems: The formation control problem treats the resultant force and the resultant moment acting on each vehicle, and the individual vehicle control problem treats the complimentary degrees-of-freedom[12]. In the illustrations found later in this thesis, the vehicles represent spherical balloons. The drag coefficients of the balloons are given by

$$C_D = 24/\mathrm{Re} + 6/(1+\sqrt{\mathrm{Re}}) + 0.4 \tag{2}$$

in which Re denotes Reynolds Number[18]. This curve fit equation is valid for $0 \le \mathrm{Re} \le 2\times10^5$. Table 1, on the following page, gives the drag coefficient for a spherical balloon for various diameters and velocities during standard day conditions.

Table 1 – Tabulated Drag Coefficient

Drag Coefficient of a Sphere for Given Diameter and Velocity							
		Velocity (ft/s)					
		5	10	15	20	25	30
Sphere Diameter (ft)	1	0.43	0.42	0.42	0.42	0.41	0.41
	2	0.42	0.42	0.41	0.41	0.41	0.41
	3	0.42	0.41	0.41	0.41	0.41	0.41
	4	0.42	0.41	0.41	0.41	0.41	0.41

Specifying the problem of formation flying, as in the above, raises questions as to an appropriate structure that best balances issues in the areas of system design, controls, electronics, and networking. How best is the system separated into components that can be designed independent of one another? What are the real-time communication requirements, and how best is this information networked?

Chapter 3

COMMUNICATION AND MEASUREMENT SIGNALS

Signals and the Sensing Truss

The network for autonomously flying vehicles consists of wireless communication signals and wireless measurement signals. The communication signals are characteristically intermittent and they can be transmitted and received with relatively low bandwidth requirements. The measurement signals are characteristically continuous in time, analog signals that require more stringent requirements in speed and bandwidth. There are two types of measurement signals of interest in formation flying – relative measurements, which are between vehicles, and inertial measurements, which are between the vehicle and the reference source (e.g., ground and GPS). The measurement process is essentially a triangulation process. Robust triangulation is best accomplished by separating the transmitters from the receivers. Well-separated transmitters and well-separated receivers maximize robustness in the presence of sensor noise. In a planar system, as shown in Fig. 1 below, 2 transmitters and 1 receiver on each of

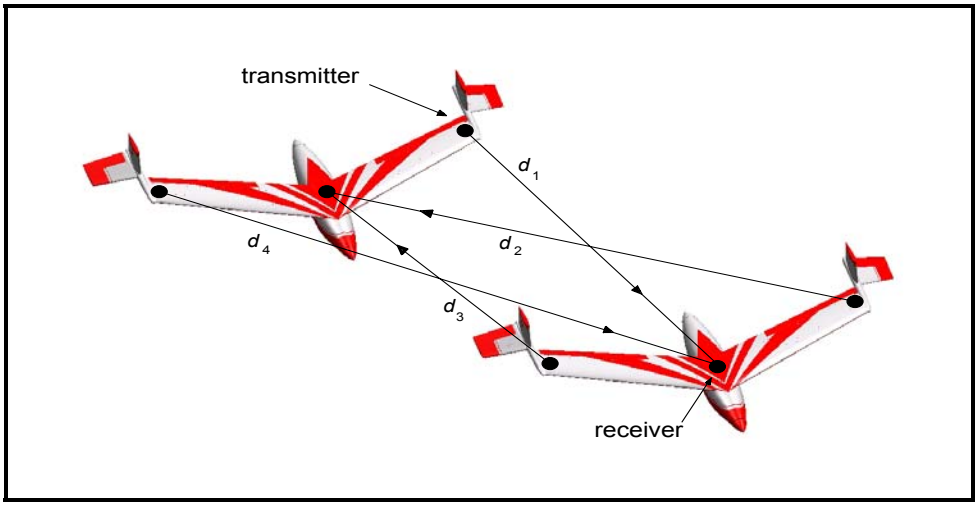

Figure 1 – 2-D Sensing Truss

the i^{th} and j^{th} vehicles fully determine the relative position and orientation of the j^{th} vehicle relative to the i^{th} vehicle and the i^{th} vehicle relative to the j^{th} vehicle. In a 3-dimensional system, 3 transmitters and 1 receiver on each of the i^{th} and j^{th} vehicles fully determine the relative position and orientation of the j^{th} vehicle relative to the i^{th} vehicle and the i^{th} vehicle relative to the j^{th} vehicle[19]. The receiving signals and the transmitting signals for the measurement process make up a **sensing truss** - possessing stability characteristics that are analogous to the stability characteristics of the corresponding structural truss.

Formation Networks

The complexity of the network is important, particularly in the event that failures occur. The methods and procedures for accommodating failures grow in complexity with the complexity of the network. The question arises to what extent the complexity of the network can be minimized. The two simplest networks are decentralized networks and nearest-neighbor networks. Decentralized networks use inertial measurements on each vehicle, eliminating the need for relative measurements, all together. Nearest-neighbor networks designate at least one vehicle as the leader and the others as the followers. The leaders receive inertial measurements and the leaders and the followers are linked by relative measurements. This thesis considers only decentralized and nearest-neighbor networks with one leader. Much more complex networks can be built from or separated into simpler units using these 2 cases as fundamental building blocks.

Figure 2(*a*), given on the following page, shows a block-diagram representation for a decentralized network. As shown, the i^{th} vehicle receives a wireless measurement of inertial position and a wireless communication from the reference source. The other elements of the block-diagram will be described later in the thesis. Figure 2(*b*), given on the following page, shows a block-diagram representation for a nearest-neighbor network. As shown, the i^{th} vehicle receives

wireless measurements from neighboring vehicles of relative positions, transmits a reference signal to neighboring vehicles, and receives a wireless communication from an external command source. If the i^{th} vehicle is the leader, a wireless measurement of inertial position is also received (not shown).

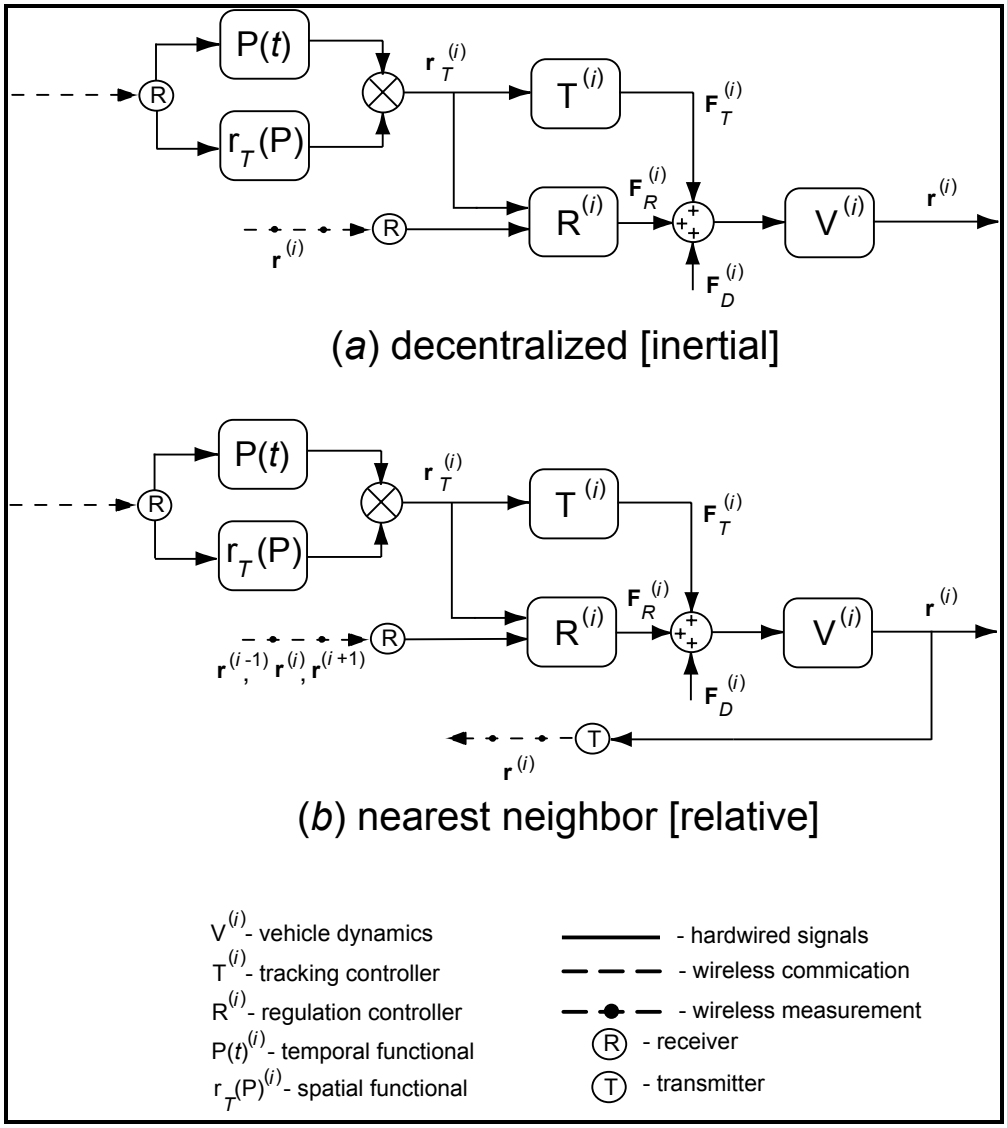

Figure 2 – Flow Diagrams for i^{th} Vehicle

Chapter 4

CHANGING THE FORMATION

Characteristics of Formation Changes

In certain applications, the interest lies in developing autonomously flying vehicles with the capability of flying in as many predetermined formations as possible. However, it is prohibitive to pre-record each possible formation change. Therefore, in order to enable the vehicles to fly in a large number of possible formations, the formations can be generated on-board from a set of **elementary formations.** The formations can be generating by superimposing elementary formations, translating and rotating the elementary formations, expanding them, etc. Figure 3*a* below shows a translation and rotation of an elementary formation, and Fig. 3*b* below shows a configuration and density change of an elementary formation. The particular formations that are commanded in this way are expressed in terms of just a few parameters.

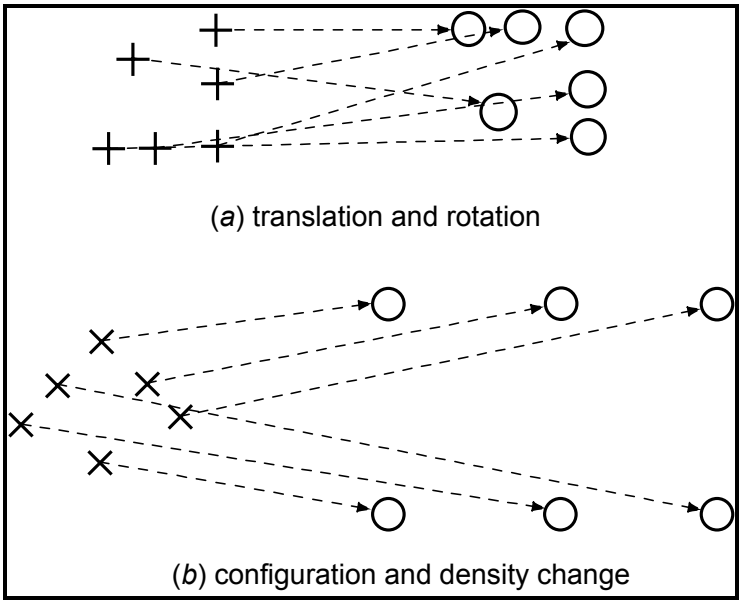

Figure 3 – Formation Changes

Separation of Tracking and Regulation Control

The formation-flying control problem is formulated below in accordance with modern control practices. The control problem is separated into a tracking problem and a regulation problem[20]. This enables the task of changing a formation and the task of maintaining a formation to be separated into processes that are designed independent of each other. The implication is that the settling time, peak-overshoot, and steady-state error requirements of the regulation problem can be met independent of the formation change requirements. The control force is expressed as

$$\mathbf{F}_C^{(i)} = \mathbf{F}_T^{(i)} + \mathbf{F}_R^{(i)} \tag{3}$$

in which $\mathbf{F}_T$ is the tracking force and $\mathbf{F}_R$ is the regulation force. The tracking force controls **formation changes** and the regulation force **maintains the formation**. This separation methodology for the i^{th} vehicle is depicted previously in Fig. 2 with the **T** and **R** blocks. The tracking control is discussed next and the regulation control will be discussed in Chapter 5.

Tracking Algorithm

Let the desired positions of the vehicles during the formation change be denoted by $\mathbf{r}_T^{(i)}$ and let the desired angular velocities of the vehicles during the formation change be denoted by $\boldsymbol{\omega}_T^{(i)}$. The open-loop tracking force and the open-loop tracking moment are then given by

$$\mathbf{F}_T^{(i)} = m_0^{(i)}\ddot{\mathbf{r}}_T^{(i)} - \mathbf{F}_{D0}^{(i)}, \qquad \mathbf{M}_T^{(i)} = I_0^{(i)}\dot{\boldsymbol{\omega}}_T^{(i)} - \mathbf{M}_{D0}^{(i)} \tag{4a,b}$$

$$\mathbf{F}_{D0}^{(i)} = -\frac{1}{2}\rho_0 V^{(i)2} S C_D \left(\frac{\mathbf{V}^{(i)}}{V^{(i)}}\right), \qquad \mathbf{M}_{D0}^{(i)} = \mathbf{0} \tag{4c,d}$$

in which $m_0^{(i)}$ and $I_0^{(i)}$ are the postulated mass and the postulated inertia matrices of the i^{th} vehicle, and $\mathbf{F}_{D0}^{(i)}$ and $\mathbf{M}_{D0}^{(i)}$ are the postulated disturbance force and the

postulated disturbance moment acting on the i^{th} vehicle (for balloons only). The postulated disturbance moment is zero for spherical balloons. Under ideal circumstances, the tracking forces $\mathbf{F}_T^{(i)}$ and the desired tracking moments $\mathbf{M}_T^{(i)}$ in Eq. (4) cause the vehicles to follow the desired paths $\mathbf{r}_T^{(i)}$ and $\boldsymbol{\omega}_T^{(i)}$.

Separation of Spatial and Temporal Controls

The desired positions $\mathbf{r}_T^{(i)}$ themselves can be separated into two components that are designed independent of each other. This is accomplished by expressing the desired position only implicitly as a function of time and explicitly as a function of space, written

$$\mathbf{r}_T^{(i)} = \mathbf{r}^{(i)}(P^{(i)}(t)) \tag{5}$$

in which $\mathbf{r}^{(i)}(P)$ denotes the spatial part and $P^{(i)}(t)$ denotes the temporal part. Differentiating Eq. (5) twice with respect to time yields

$$\ddot{\mathbf{r}}_T^{(i)} = \mathbf{r}''^{(i)}\dot{P}^{2(i)} + \mathbf{r}'^{(i)}\ddot{P}^{(i)} \tag{6}$$

where primes denote derivatives with respect to P and over-dots represent derivatives with respect to t. Equation (6) is substituted into Eq. (4) for the generation of the tracking forces. The separation of the tracking force into spatial and temporal parts simplifies the command architecture of the formation. This separation enables the temporal aspects of the formation change (e.g., rapid/slow) to be separated from the spatial aspects of the formation change (e.g., particular initial formation and final formation) reducing the on-board formation data to a listing of elementary formations. Further, the communication between vehicles required for a formation change can be composed of just a few parameters. For example, in a two-dimensional straight formation change, Eq. (5) becomes

$$\mathbf{r}^{(i)}(P) = \mu^{(i)}\mathbf{r}_1^{(i)} + \tau^{(i)}\mathbf{r}_2^{(i)}, \qquad \mu^{(i)} + \tau^{(i)} = 1,$$
$$P(t) = 3\left(\frac{t}{T}\right)^2 - 2\left(\frac{t}{T}\right)^3 \tag{7a-c}$$

in which $\mathbf{r}_1^{(i)} = [x_1^{(i)} y_1^{(i)} z_1^{(i)}]^T$ and $\mathbf{r}_2^{(i)} = [x_2^{(i)} y_2^{(i)} z_2^{(i)}]^T$ denote the initial position and the final position of the i^{th} vehicle in the formations, and where T denotes the period of the formation change. For the purposes of collision avoidance, it can become necessary during the formation change to follow paths that are not straight. For example, a suitable parameterized planar parabolic formation change is, shown in Fig. 4 below, and given by

$$\mathbf{r}^{(i)}(P) = \mathbf{r}_1^{(i)} + \begin{bmatrix} x_2^{(i)} - x_1^{(i)} & y_1^{(i)} - y_2^{(i)} \\ y_2^{(i)} - y_1^{(i)} & x_2^{(i)} - x_1^{(i)} \end{bmatrix} \begin{pmatrix} P \\ 4qP(1-P) \end{pmatrix}, \qquad 0 \le P \le 1 \tag{8}$$

where $\mathbf{r}_1^{(i)} = [x_1^{(i)} y_1^{(i)}]^T$ is the position of the i^{th} vehicle in the initial formation, $\mathbf{r}_2^{(i)} = [x_2^{(i)} y_2^{(i)}]^T$ is the position of the i^{th} vehicle in the final formation, and where q is parabolic eccentricity, which represents the ratio of the height to the length of the parabolic path. It should also be noted that there are many ways to specify the temporal and spatial functions of the vehicles, depicted in Eq. (5), such as using n^{th} order time functions and splines. However, the more complex the temporal and spatial functions are the more information that must be transmitted between vehicles.

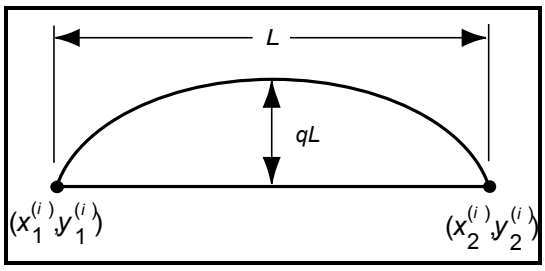

Figure 4 – Planar Parabolic Formation Change

Chapter 5

MAINTAINING THE FORMATION

The regulation problem is a full-dimensional control problem in which the number of control inputs is the same as the number of degrees-of-freedom. The regulation problem can be formulated as an optimal control problem, as a decentralized control problem, as an independent modal space control problem, or as a robust control problem[20]. Regardless of the manner in which the problem is formulated, it can be shown that the most effective full-dimensional control is decentralized, while the modes are controlled independent of each other, while the control is insensitive to errors in the physical parameters, and while the dynamic performance is globally optimal[8]. These results suggest that the formation-flying problem should be formulated either as a decentralized control problem or as a nearest-neighbor control problem depending on the types of sensors that are used. Decentralized control can be implemented when each vehicle is equipped with inertial sensors and nearest neighbor control can be implemented when one or more of the vehicles (the leaders) is equipped with inertial measurements and the remaining vehicles (the followers) are equipped with relative measurements. Since nearest neighbor control uses relative measurements, and since relative measurements can also be used for collision avoidance, nearest neighbor control represents an important option to consider.

Decentralized Control

The use of decentralized control raises questions associated with the global behavior of the formation and the fuel optimality of the control, given that decentralized control is a constrained form of coupled control. It has been shown in previously cited references, however, that uniform damping of the associated modes of vibration of the system can be implemented in a decentralized manner,

that uniform damping is fuel optimal, that uniform damping does not require knowledge of the modal behavior of the system, and that uniform damping possesses several other attractive characteristics associated with its robustness. The control algorithms associated with uniform damping can also be expressed in terms of just a few parameters.

First consider the decentralized implementation of uniform damping. The uniform damping control and stiffening regulation algorithm is[14]

$$\mathbf{F}_R^{(i)} = -2\alpha m^{(i)}\left(\dot{\mathbf{r}}^{(i)} - \dot{\mathbf{r}}_T^{(i)}\right) - \left(\alpha^2 + \beta^2 - \omega^{(i)2}\right) m^{(i)}\left(\mathbf{r}^{(i)} - \mathbf{r}_T^{(i)}\right) \tag{9}$$

in which α denotes the uniform closed-loop decay rate of the vehicles, β denotes the uniform closed-loop frequency of oscillation of the vehicles, and $\omega^{(i)}$ denotes the open-loop frequency of oscillation of the i^{th} vehicle. In the case of spherical balloons, the open-loop frequencies are zero. The closed-loop decay rates can be selected to dampen 90% of the error over the settling time T_s, in which case the closed-loop decay rate is expressed in terms of the settling time as $\alpha = \ln(10)/T_s$. The closed-loop response of the i^{th} vehicle is then

$$\mathbf{u}^{(i)} = e^{-\alpha t}\left\{\mathbf{u}_0^{(i)}\cos(\beta t) + \frac{1}{\beta}\left[\dot{\mathbf{u}}_0^{(i)} + \alpha\mathbf{u}_0^{(i)}\right]\sin(\beta t)\right\} \tag{10}$$

in which $\mathbf{u}^{(i)} = \mathbf{r}^{(i)} - \mathbf{r}_T^{(i)}$ is the displacement error vector of the i^{th} vehicle. Holding the settling time constant, it can be shown that the control effort $C^{(i)} = \int_0^\infty \left|\mathbf{F}_R^{(i)}\right|^2 dt$ associated with the i^{th} vehicle is minimized when the closed-loop frequency of that vehicle is identical to its open-loop frequency[9]. The control effort increases as the difference between the closed-loop frequency and the open-loop frequency increases. The determination of the closed-loop frequency is driven by peak-overshoot requirements, which in turn depend on an

admissible set of disturbances. The uniform decay rate α can be determined from the settling time requirements independent of the peak-overshoot requirements and the uniform closed-loop frequency β can be determined from the peak-overshoot requirements independent of the settling time requirements. The decentralized control problem formulated above is also extremely robust. It can be shown that the stability of the vehicles is independent of the physical properties of the vehicles.

Nearest Neighbor Control

Using nearest neighbor control, the designer's first task is to specify the connectivity between the vehicles, i.e., the nearest neighbors. Furthermore, the designer needs to specify the leaders and the followers. The leaders are the vehicles equipped with inertial measurements. The followers are equipped with relative measurements between nearest neighbors (connectivity). Consider the case in which there is one leader. Let the leader be designated by the subscript 1 and the followers designated by the subscripts 2, 3, … , 3*n*. The associated connectivity matrix is $\mathbf{C}(i,j)$, $(i, j = 1, \ldots, 3n)$ in which the i^{th} row is associated with the i^{th} vehicle, the j^{th} entry in the i^{th} row is 1 (or 0) if the j^{th} vehicle can (or can not) measure relative to the i^{th} vehicle. The number of 1's in the matrix represents the number of one-way connections. Note that it is not necessary that **C** be symmetric, i.e., a designer can design a j^{th} vehicle that can measure relative to the i^{th} vehicle while the i^{th} vehicle can not measure relative to the j^{th} vehicle (e.g., vehicles that can only see ahead and not behind). However, when **C** is symmetric, the connections are each two-way and the feedback control can emulate a mass-spring-damper system. The nearest neighbor linear regulation algorithm can be expressed as

$$\mathbf{F}_R = -G_R\left(\mathbf{r} - \mathbf{r}_T\right) - H_R\left(\dot{\mathbf{r}} - \dot{\mathbf{r}}_T\right) \tag{11}$$

in which $\mathbf{r} = [\mathbf{r}^{(1)T}\ \mathbf{r}^{(2)T}\ \ldots\ \mathbf{r}^{(n)T}]^T$ is the configuration vector of the formation, $\mathbf{r}_T = [\mathbf{r}_T{}^{(1)T}\ \mathbf{r}_T{}^{(2)T}\ \ldots\ \mathbf{r}_T{}^{(n)T}]^T$ is the desired position of the formation, $\mathbf{F}_R = [\mathbf{F}_R{}^{(1)T}\ \mathbf{F}_R{}^{(2)T}\ \ldots\ \mathbf{F}_R{}^{(n)T}]^T$ is the control force vector of the formation, and G_R and H_R are $3n$ x $3n$ symmetric displacement gain and velocity gain matrices. In two dimensions G_R and H_R are $2n$ x $2n$.

The vehicles can be connected in a variety of ways; the best way to connect the vehicles is a matter of optimization. The connectivity matrix is associated with a specific pair of initial and final formations, each of which could be constructed from elementary formations. For a given pair of initial and final formations, another consideration is associated with the "stiffness" of the associated connectivity. As a follower is connected to the leader through more intermediary vehicles, its inertial position is known with less accuracy, and the control of the motion of that vehicle based on relative information alone becomes more and more difficult. To circumvent this problem, the number of connections between the vehicles can be increased and/or the number of leaders can be increased. For example, an open chain is closed in Fig. 5 below.

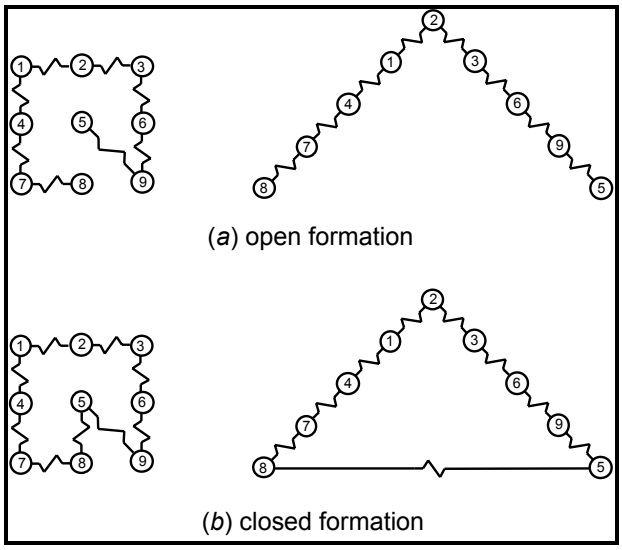

Figure 5 - Open and Closed Connectivity

Of course, an increase in the number of connections and an increase in the number of leaders accompany increases in measurement complexity.

Substituting Eq. (11) into Eqs. (1), yields the closed-loop system

$$M\ddot{\mathbf{u}} + H_R\dot{\mathbf{u}} + G_R\mathbf{u} = \mathbf{F}_D \tag{12}$$

in which M is the symmetric mass matrix of the formation, $\mathbf{u} = \mathbf{r} - \mathbf{r}_T$ is the displacement error vector of the formation, and $\mathbf{F}_D = [\mathbf{F}_D{}^{(1)T}\ \mathbf{F}_D{}^{(2)T}\ \ldots\ \mathbf{F}_D{}^{(n)T}]^T$ is the disturbance force vector of the formation. The symmetric nearest-neighbor control problem formulated above is extremely robust. It can be shown that global stability of the vehicles is guaranteed for positive control gains, independent of the physical properties of the vehicles.

Perturbation Analysis for Nearest Neighbor Control

The question arises how to select the control gains in Eq. (12). The goal is to select control gains that uniformly dampen the motion to the extent possible, recognizing that uniform damping of the modes minimizes the required control authority of the actuation and maximizes the global dynamic performance of the formation. The nearest neighbor control is constrained by the connectivity, which complicates the problem. To overcome this, first express the control gains as

$$G_R = \sum_{k=1}^{N} g_k B_k \quad \text{and} \quad H_R = \sum_{k=1}^{N} h_k B_k \tag{13a,b}$$

in which g_k and h_k, (k = 1, 2, … ,N), denote positive control gains and B_k is the connectivity matrix associated with the k^{th} two-way connection. Stability is guaranteed provided $g_k > 0$ and $h_k > 0$ regardless of the physical parameters of the vehicles. A first-order perturbation analysis can be used in order to accurately calculate the control gains, as the following shows. The eigenvalue problem

associated with Eq. (13) is $[s_r^2 M + s_r H_R + G_R]\boldsymbol{\varphi}_r = 0$, in which s_r is the r^{th} system eigenvalue and $\boldsymbol{\varphi}_r$ is the r^{th} system eigenvector. The eigenquantities can be expressed as[21]

$$s_r = s_{0j} + s_{1j}, \quad \boldsymbol{\varphi}_j = \boldsymbol{\varphi}_{0j} + \boldsymbol{\varphi}_{1j}, \quad G_R = G_{R0}, \quad H_R = H_{R1} \tag{14}$$

in which 0 denotes a nominal quantity and 1 indicates a perturbation. Notice that the displacement gain matrix is regarded as a nominal quantity and that the velocity control gain matrix is regarded as a perturbation. The nominal system is the symmetric mass-spring system and the perturbed system includes the damping. This division of responsibilities enables the peak-overshoot requirements and the settling time requirements in the nearest neighbor control problem to become separated. The displacement control gain matrix is first determined to satisfy the peak-overshoot requirements followed by the determination of the velocity control gain matrix to satisfy the settling time requirements, which will be done momentarily. Substituting the eigenquantities in Eq. (14) into the eigenvalue problem, pre-multiplying the result by $\boldsymbol{\varphi}_{0i}^T$, invoking the modal orthonormality conditions ($\boldsymbol{\varphi}_{0i}^T M \boldsymbol{\varphi}_{0j} = \delta_{ij}$ and $\boldsymbol{\varphi}_{0i}^T G_R \boldsymbol{\varphi}_{0j} = \beta_r^2 \delta_{ij}$), and neglecting second- and higher-order terms, yields

$$\alpha_i = \frac{1}{2} \boldsymbol{\varphi}_{0i}^T H_R \boldsymbol{\varphi}_{0i} \tag{15}$$

in which $s_{0i} = i\beta$, and $s_{1i} = -\alpha_i$ so α_i denotes the closed-loop decay rate of the i^{th} mode of the system. Equation (15) is a set of linear algebraic equations. The number of equations is equal to the number of degrees of freedom $3n$ ($2n$ for 2-dimensional systems) and the number of unknowns N is equal to the number of connections. Substituting Eq. (13b) into Eq. (15) yields

$$\boldsymbol{\alpha} = D\mathbf{h}, \qquad D_{ik} = \frac{1}{2}\boldsymbol{\varphi}_{0i}^{T} B_k \boldsymbol{\varphi}_{0i} \tag{16a,b}$$

in which $\boldsymbol{\alpha} = [\alpha_1 \ \alpha_2 \ldots \ \alpha_{3n}]^T$ is the $3n$-dimensional vector of approximate modal decay rates and $\mathbf{h} = [h_1 \ h_2 \ldots h_N]^T$ is the N-dimensional vector of velocity feedback gains that we wish to determine. In the following, the matrix D is assumed to be full rank without loss of generality[1]. When the number of degrees of freedom is less than or equal to the number of connections, the weighted minimum norm solution of Eq. (16) is $\mathbf{h} = W^{-1}D^T(DW^{-1}D)^{-1}\boldsymbol{\alpha}$ in which W is a N x N weighting matrix and the weighted norm squared is $J = \mathbf{h}^T W \mathbf{h}$. When the number of equations is equal to the number of connections, a simple inverse of Eq. (16) yields the solution $\mathbf{h} = D^{-1}\boldsymbol{\alpha}$. When the number of degrees of freedom is greater than the number of connections, no exact solution to Eq. (16) exists and we resort to approximate solutions. As described later, this case arises from the desire to limit the number of connections, which arises from the desire to limit the number of signals detected by the wireless receivers on the vehicles. There are several possible approximate solutions to Eq. (16) that can be obtained. The weighted least squares solution, given by $\mathbf{h} = (D^T W D)^{-1} D^T W \boldsymbol{\alpha}$ minimizes the weighted error $e = (D\mathbf{h} - \boldsymbol{\alpha})^T W (D\mathbf{h} - \boldsymbol{\alpha})$. More than minimizing the error, solutions can be obtained that also penalize solutions that deviate from uniform damping. Consider the functional

$$J = (\alpha \mathbf{1} - \boldsymbol{\alpha})^T W_\alpha (\alpha \mathbf{1} - \boldsymbol{\alpha}) + \mathbf{h}^T W_h \mathbf{h} \tag{17}$$

where $\mathbf{1} = [1 \ 1 \ \ldots \ 1]^T$, W_α is a $3n$ x $3n$ weighting matrix associated with the non-uniformity of the decay rates and W_h is a N x N weighting matrix associated with

[1] If D is not full rank, the results below can be modified using a singular-value-decomposition, but for brevity this modification is omitted from the discussion below[22].

the control effort. The first term in Eq. (17) is a penalty associated with non-uniform damping and the second term penalizes the control effort. Minimization of Eq. (17) yields

$$\mathbf{h} = \alpha[D^T W_\alpha D + W_h]^{-1} D^T W_\alpha \mathbf{1} \tag{18}$$

The control gains for nearest neighbor control are determined in two independent steps. The displacement feedback gains are first determined based on peak-overshoot requirements and then the velocity feedback gains are determined based on settling-time requirements according to Eq. (18).

Chapter 6

NUMERICAL RESULTS

The following illustration consists of an initial planar 3 by 3 grid of 9 balloon vehicles which changes into a planar V-shaped formation. The number of degrees of freedom is 18 ($n = 9$). MATLAB™ was used for all computations and to plot the outputs. This code is given on a CD-R which is attached to the inside back cover of this thesis. The readme.txt file on this CD-R gives the hierarchy of the files.

The tracking problem is first treated. Straight formation changes were first attempted and vehicles 5 and 9 nearly (see Fig. 5 for numbering convention) collided during the formation change. Parabolic formation changes were then developed using the principle of separating the spatial and the temporal functions for the formation change, as shown in Fig. 6 on the following page.

To avoid collisions, the parabolic eccentricities were specified to be $q_1 = q_2 = q_3 = q_4 = q_6 = q_8 = 0$, $q_5 = -0.2$, $q_7 = -0.1$, and $q_9 = 0.1$. Although not performed here, the parabolic eccentricities could be determined more optimally to maximize the separation between the vehicles over the time of the formation change and the lengths of the associated arcs. Also, notice that the actual paths of the vehicles and the desired paths of the vehicles are coincident in Fig. 6 because no disturbances have been introduced yet.

Next, a wind disturbance is introduced and the combined tracking and regulation problem is treated.

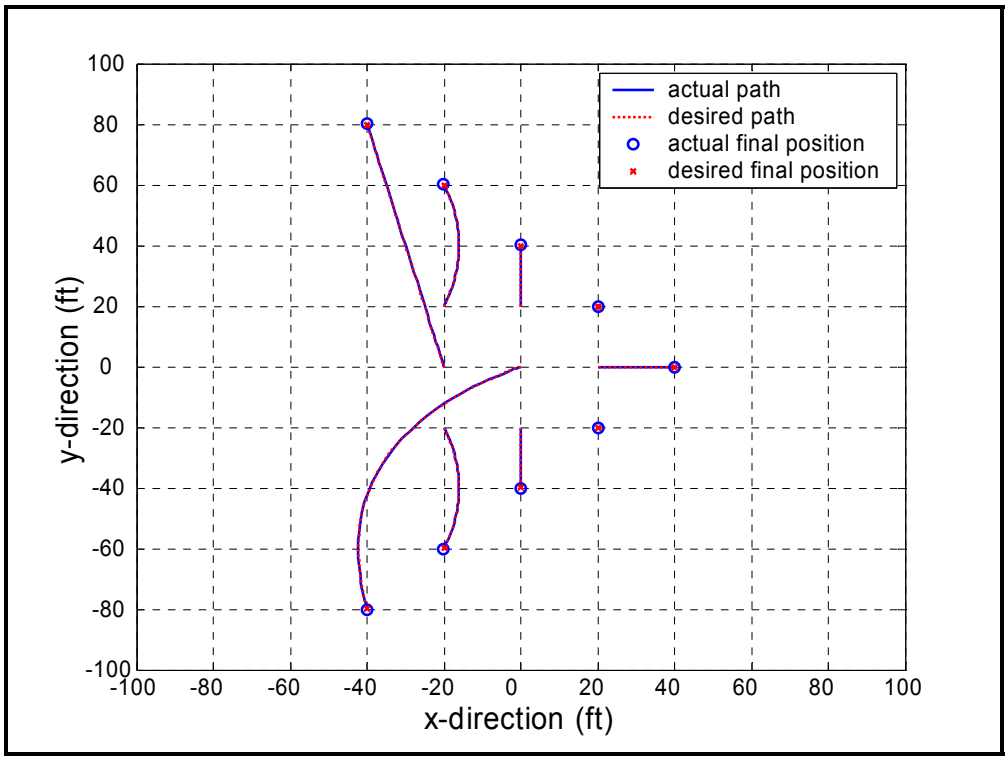

Figure 6 – Ideal Open-loop Formation Change

Decentralized Network

As mentioned earlier, the closed-loop frequency is determined by peak-overshoot requirements, which in turn depend on an admissible set of disturbances. As shown in Fig. 7 on the following page, the control effort $C^{(i)} = \int_0^\infty \left|\mathbf{F}_R^{(i)}\right|^2 dt$ increases with the settling time, so the closed-loop frequency selected is the lowest one that meets the peak-overshoot requirements.

For the purposes of this illustration, assume that the nominal separation distance is Δ, that it is desirable to reject a wind disturbance of v_n, and that the associated minimum separation distance is $n\Delta$, so the wind force is $F_w = \frac{1}{2}\rho_0 v_w^2 S C_D = g(n\Delta)$ in which g denotes the displacement feedback control

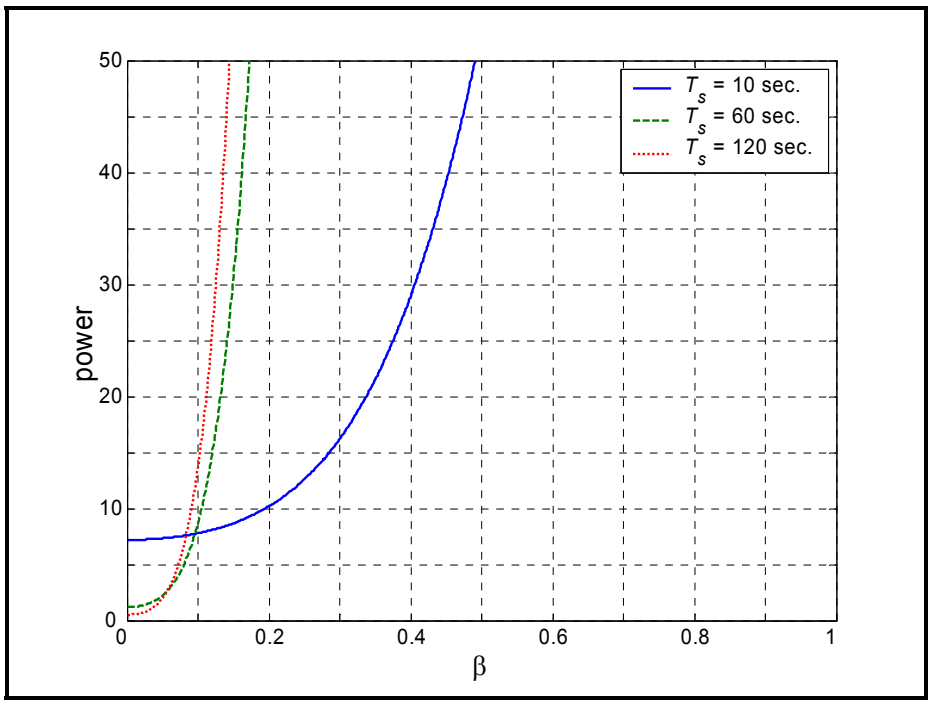

Figure 7 – Power versus Closed-loop Frequency

gain of the decentralized regulation feedback. It follows that

$$g = \frac{1}{2}\frac{\rho_0 v_w^2 S C_D}{n\Delta} \tag{19}$$

Figure 8 on the following page shows a formation change in which a wind gust has occurred when the formation change was initiated. The settling time for the regulation was set equal to the time period of formation change. Thus, the formation change is completed when 90% of the error between the desired path and the actual path has been eliminated. Notice the angle on the wind, and the overshoot of the error. The damping factor of the fundamental mode of the system is 0.39.

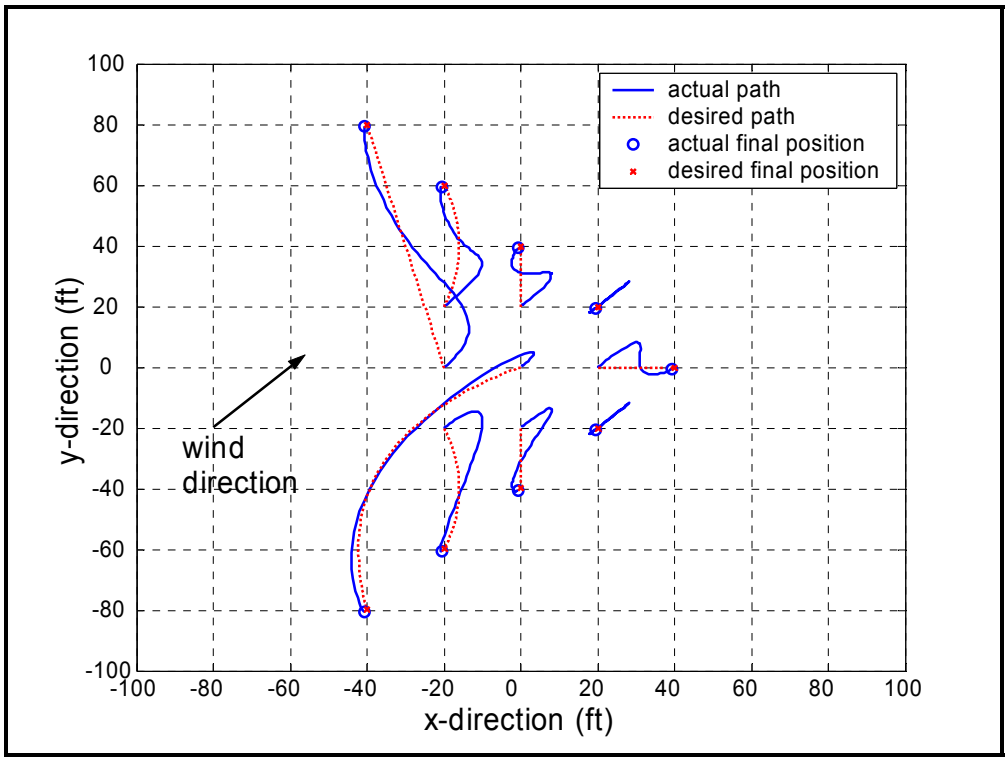

Figure 8 – Decentralized Formation Change in an Initial Wind Gust

Nearest Neighbor Network

In this illustration, $W_\alpha = I_{3n}$ (the identity matrix) and $W_\eta = \eta I_N$ in Eq. (17). The formation was connected in two ways – using an open formation and a closed formation (as depicted in Figs. 5*a* and 5*b*). Vehicle 2 is the leader and the rest of the vehicles are followers. The displacement feedback gains in the open formation and the closed formation, which were determined from Eq. (19), are g_k = 0.05 for each k^{th} connection. The velocity feedback gains were determined from Eq. (18), which is a linear approximation. The accuracy of the approximation was first examined in Fig. 9 over a range of damping factors. In Fig. 9, $\boldsymbol{\alpha}_e$ is the vector of exact decay rates that are obtained from the closed-loop eigenvalue problem associated with Eq. (12), and ω_f denotes the fundamental

frequency of the system. Figure 9 shows that the approximation is accurate over the damping ratios α/ω_f of interest.

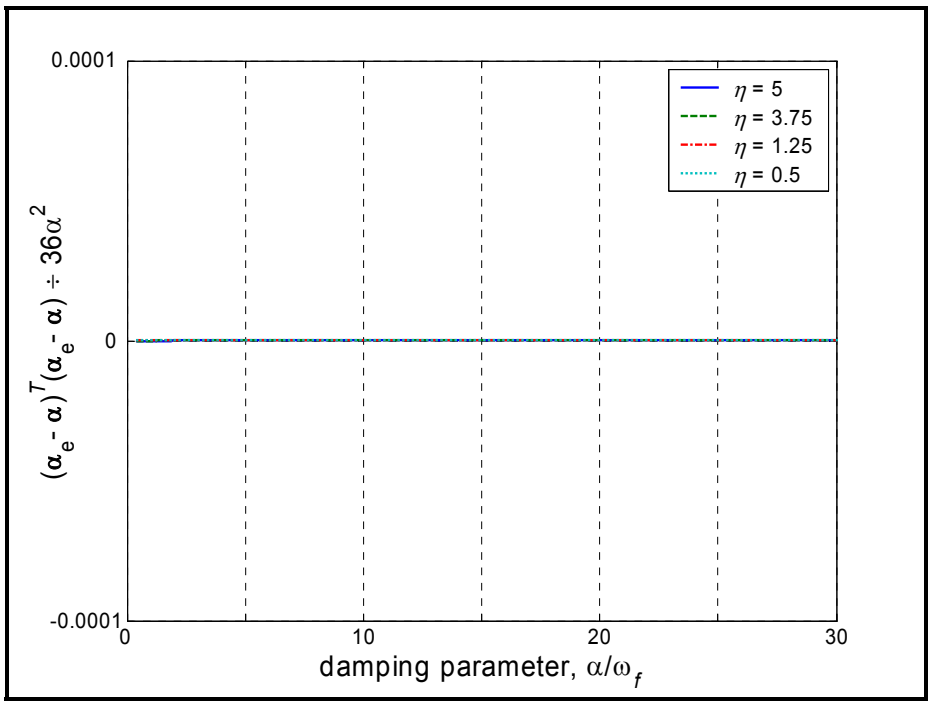

Figure 9 – Verification of Accuracy of Perturbation Analysis (Open)

In this illustration the number of connections is less than the number of degrees of freedom, resulting in an inability to obtain uniform damping of all the modes of vibration. The level of non-uniformity of the decay rates was examined over a range of damping ratios and for different weighing parameters η. As shown in Fig. 10, on the following page, the level of non-uniformity does not depend on the damping ratio, and it increases with η.

Figure 11, also shown on the following page, shows the control effort over a range of damping ratios and for different weighing parameters η. Like the non-uniformity in Fig. 10, the control effort does not depend on the damping

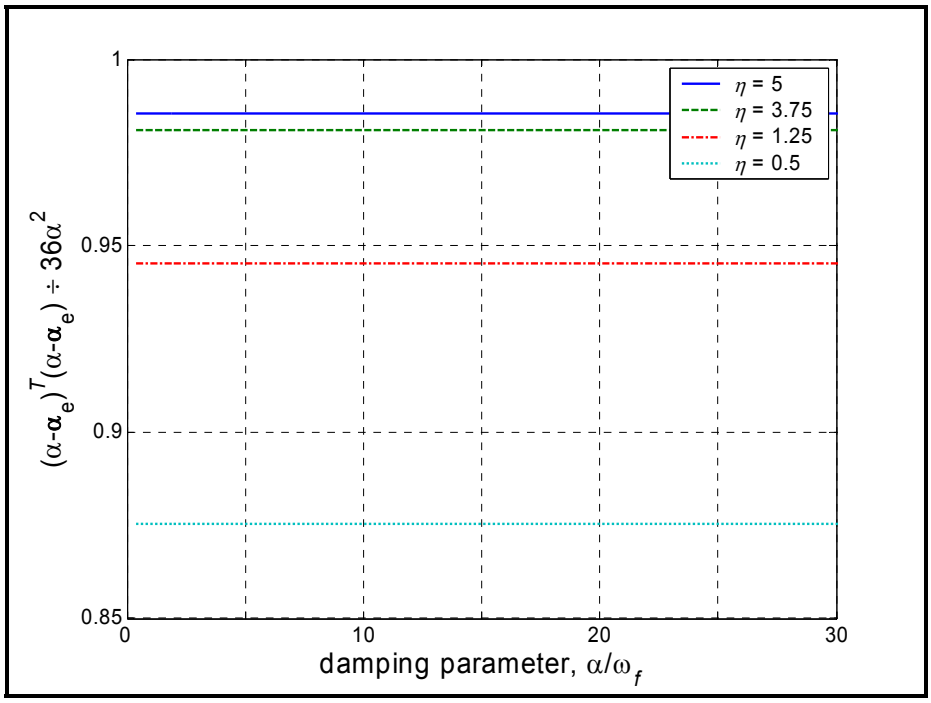

Figure 10 – Non-Uniformity Part of Functional *J*

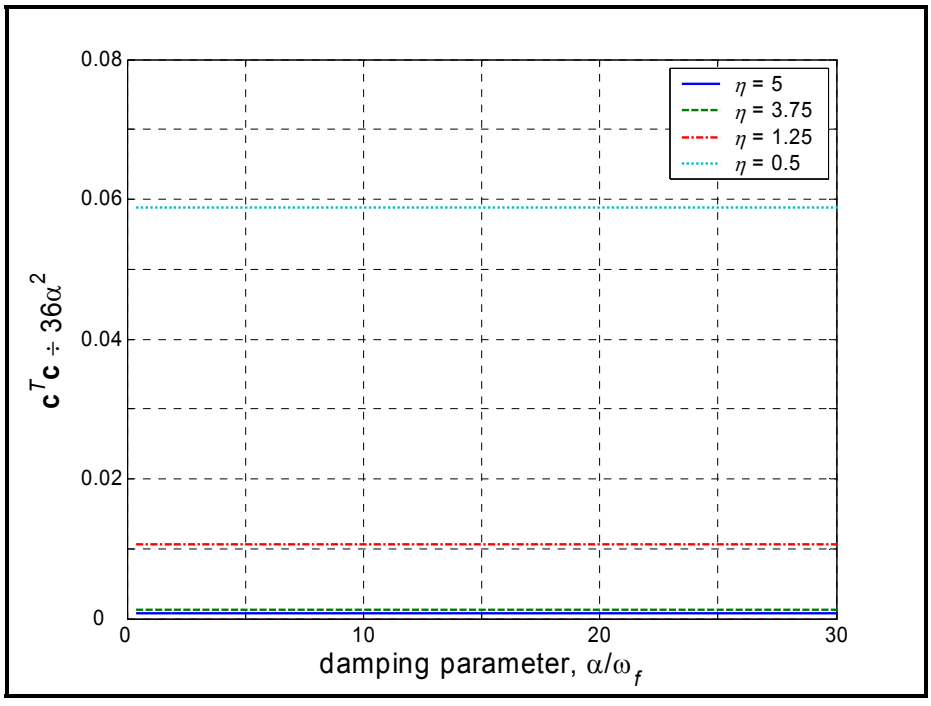

Figure 11 – Cost in Gain Part of Functional *J*

ratio, but it decreases with increasing η. The trends exhibited for the open formation in Figs. 9 and 10 are the same trends that are exhibited for the closed formation.

Figures 12 and 13, shown below, shows that there is a practical non-zero minimum level of non-uniformity that is attainable, even when the control effort is allowed to increase to a prohibitively large level. The limit is a result of the physical limitations associated with using fewer connections than degrees of freedom. Although not shown, the non-uniformity in this illustration is dominated by the lowest mode of vibration, which damps out at a lower rate than the other modes.

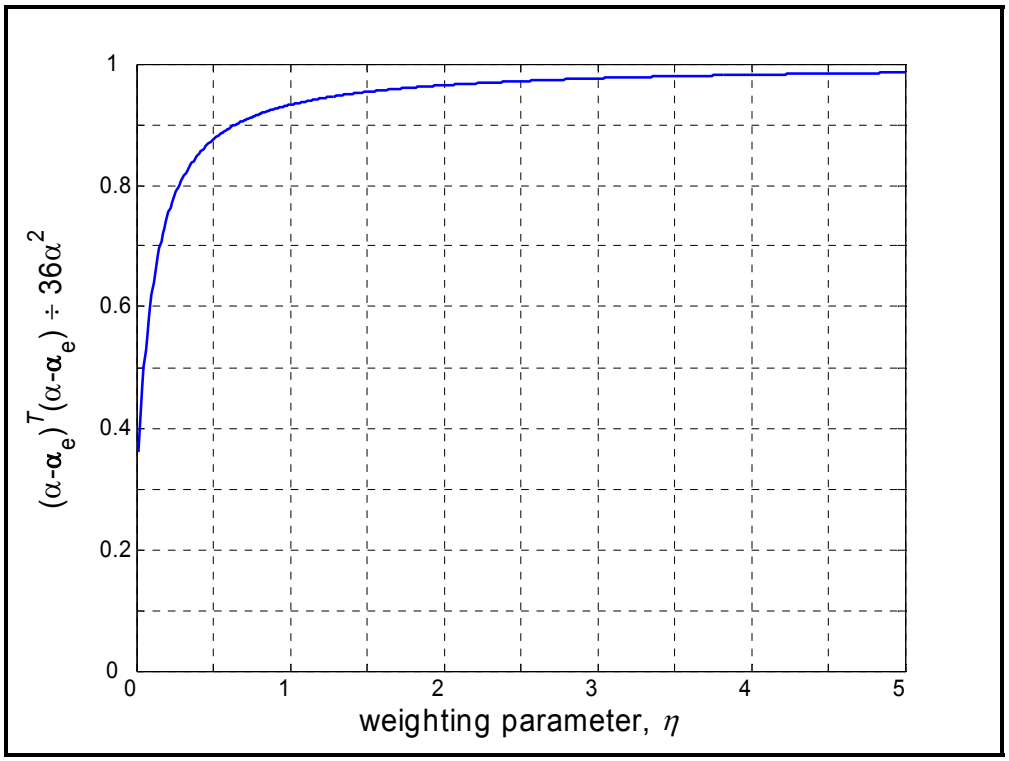

Figure 12 – Weighting Parameter (Open)

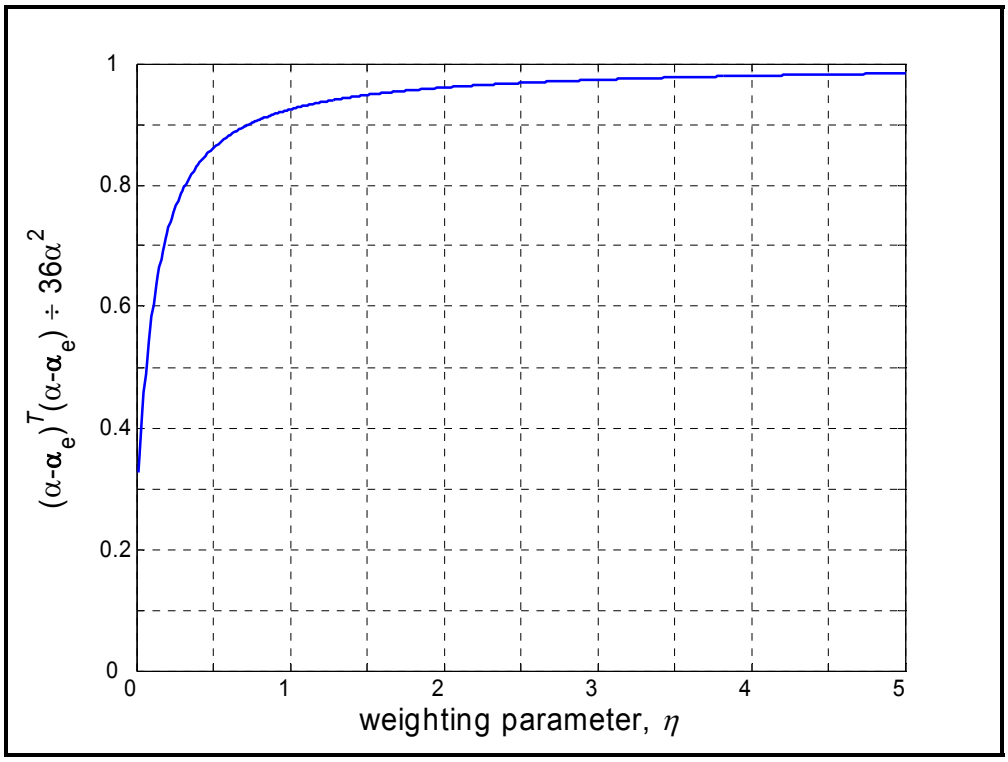

Figure 13 – Weighting Parameter (Closed)

Figure 14, shown on the following page, shows a formation change in which a wind gust has occurred when the formation change was initiated. The strength of the wind gust in Fig. 14 was 177% lower than in Fig. 8 although the overshoot experienced in Fig. 14 is similar to the overshoot found in Fig. 8. In fact, when the strength of the wind gust was taken to be the same as in Fig. 8, the overshoot in the response was considerably greater than the overshoot experienced in Fig. 8. The explanation for the increase was traced to the measurement system. The overshoot on the follower vehicles was found to increase with their separation from the leader. Notice in Fig. 14 that the deviation of the final positions of the vehicles from the desired positions increases as the vehicles are farther from the leader. The relative displacement and velocity measurements became less effective feedback variables as they are located further back in the formation.

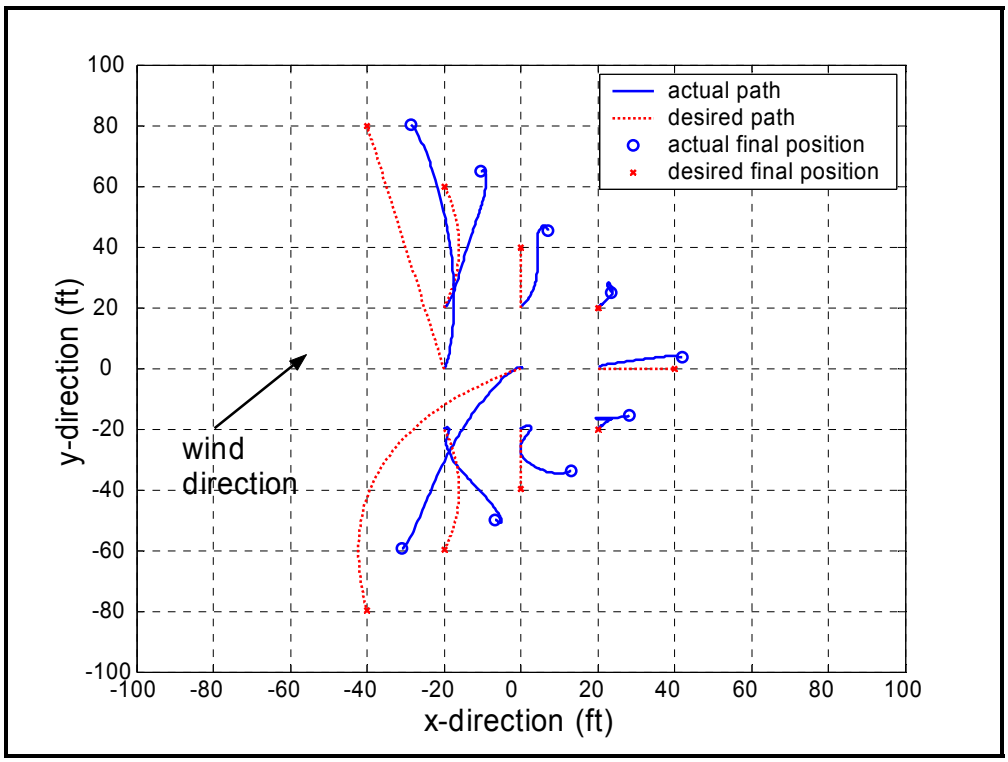

Figure 14 – Nearest-Neighbor Formation Change in an Initial Wind Gust (Open)

Chapter 7

SUMMARY AND CONCLUSIONS

This thesis developed an autonomous control approach for aerospace vehicle formations that balanced important design issues in controls, electronics, communications, robustness, fuel consumption, and global dynamic performance. The thesis focused on the inherent inter-dependences that exist in the design process and the ways in which they are handled to reduce overall design complexity. The thesis employed separation principles between: (a) signal transmission and reception, (b) tracking and regulation, (c) spatial and temporal tracking, (d) stiffening and damping, and (e) feedback connections (decentralized or nearest-neighbor).

The thesis developed two viable approaches; one was referred to as decentralized control and the other was referred to as nearest neighbor control. Decentralized control would be the preferred of the two approaches when the weight requirements of the inertial sensors are satisfied (which is critical in micro-aerial vehicles) and when a reference source is available nearby, i.e., when a reference signal of sufficiently low noise is available. The nearest neighbor control would be preferred when multiple reference signals having sufficiently accurate relative measurements are not available. In general, the decentralized control approach is suited to short-distance problems and the nearest-neighbor approach is suited to the long-distance problems.

The thesis also introduced several topics that would benefit from further analysis. Elementary formations that possess attractive properties have not been developed, nor a strategy for vehicle connectivity that minimizes the tracking paths and maximizes the separation distances between the vehicles. This thesis

also confined itself to two-way connections and single leaders; the viability of one-way connections and multiple leaders are open questions.

BIBLIOGRAPHY

[1]M. J. Balas (1978) "Active Control of Flexible Systems," *J. Optimization Theory and Applications*," Vol. 25, No. 3, p. 415-436.

[2]L. Meirovitch and H. Baruh (1982) "Control of Self-Adjoint Distributed-Parameter Systems," *J. Guidance, Control, and Dynamics,* Vol. 5, Jan.-Feb., p. 60-66.

[3]A. Arbel and N. K. Gupta (1981) "Robust Collocated Control for Large Flexible Space Structures," *J. Guidance, Control, and Dynamics*, Sept.-Oct., p.480-486.

[4]A. Hale and G. A. Rahn (1984) "Robust Control of Self-Adjoint Distributed-Parameter Systems," *J. Guidance, Control, and Dynamics*, Vol. 7, p. 265-273.

[5]H. Baruh and L. Silverberg, (1985) "Robust Natural Control of Distributed Systems," *J. Guidance, Control and Dynamics*, Vol. 8, No. 6, Nov.-Dec.

[6]R. A. Calico and W. T. Miller (1983), "Decentralized Control of Distributed-Parameter Systems," *AIAA Paper 82-1404*, Aug.

[7]L. Meirovitch and L. Silverberg (1983) "Globally Optimal Control of Distributed Systems," *Journal of Optimal Control Applications and Methods*, Vol. 4, 365-386.

[8]L. Silverberg (1985) "Uniform Damping Control of Spacecraft," *J. Guidance, Control and Dynamics*. Vol. 9, No. 2, March-April, p. 221-227

[9]L. Silverberg and M. Morton (1989) "On the Nature of Natural Control," *J. Vibration, Acoustics, Stress and Reliability in Design*, Vol. 111, Oct., p.412-422.

[10]L. Silverberg (1990) "Motion Control of Space Structures," *J. Aerospace Engineering*, October, Vol. 3, No. 4, Oct., p. 223-234.

[11]L. Silverberg, J. Redmond, and L. Weaver, Jr. (1992) "Uniform Damping Control: Discretization and Optimization," *J. of Applied Mathematical Modeling*, Vol. 16, No. 3, March, pp. 133-140.

[12]H. Baruh and L. Silverberg, (1988) "Simultaneous Maneuver and Vibration Suppression of Flexible Spacecraft," *Journal of Applied Mathematical Modeling*, Vol. 12, No. 6, Dec., p. 546-555.

[13]L. Silverberg and L. A. Foster (1990) "Decentralized Feedback Maneuver of Flexible Spacecraft," *Journal of Guidance, Control and Dynamics*, Vol. 13, No. 2, March-April 1990, p. 258-264.

[14]L. Silverberg and G. Washington (1997) "Uniform Damping and Stiffness Control of Structures with Distributed Actuators," *J. Dynamic Systems, Measurement and Control*, Vol. 119, No. 3, Sept., pp. 561-565.

[15]L. Silverberg and G. Washington (1999) "Weighted-Residual Discretization for Uniform Damping and Uniform Stiffening of Structural Systems, *J. Guidance,*

Control, and Dynamics, Vol. 22, No. 4, July - August, p. 614-618.
[16]J. D. Wolfe, D. F. Chichka, and J. L. Speyer, (1996) "Decentralized Controllers for Unmanned Aerial Vehicle Formation Flight," *AIAA-96-3833*.
[17]M. Pachter, J. J. D'Azzo, A. W. Proud (2001) "Tight Formation Flight Control*," J. Guidance, Control, and Dynamics*, Vol. 24, No. 2, pp. 246-254.
[18]F. M. White (1974), "Viscous Fluid Flow," *McGraw-Hill Book Co.*
[19]Communications with V. Perez, Systems Programmer, Mechanical and Aerospace Engineering, North Carolina State University, Raleigh, NC 27695-7901.
[20]L. Meirovitch (1990) "Dynamics and Control of Structures," *John Wiley and Sons, Inc.*
[21]L. Meirovitch (1997), "Principles and Techniques of Vibrations," *Prentice-Hall, Inc.*, Upper Saddle River, NJ 07458.
[22]C. L. Lawson and R. Hanson (1974), "Solving Least Squares Problems," *Prentice-Hall, Inc.*, Englewood Cliffs, NJ.